

Lattice thermal conductivity of cold-worked noble-metal alloys between 0.5 and 4 K*

A. Kapoor, J. A. Rowlands, and S. B. Woods

Department of Physics, University of Alberta, Edmonton, Alberta, Canada

(Received 9 July 1973)

Thermal-conductivity measurements were made for two Cu-, two Au-, and one Ag-based polycrystalline rods and one Cu-based single-crystal rod in the temperature range 0.5 to 4 K. The polycrystalline rods were measured with each rod first being in a highly cold-worked condition and then in various stages of recovery brought about by annealing at temperatures up to 1000 K. From the total measured conductivity, the lattice conductivity was extracted by calculating the electronic component using the Wiedemann-Franz law and electrical-resistivity measurements. In all the cold-worked alloys, the lattice conductivity did not have the temperature dependence expected from standard theory. Comparable experimental results, which have been published only for Cu alloys and only above 1.5 K are in agreement with our results. The measurements below 1.5 K indicated an even larger departure from standard theory. In the entire temperature region (0.5 to 4 K), our belief is that the anomalies are contained in that part of the lattice conductivity which is limited by dislocation scattering. The anomalies in the Ag- and Au-based alloys, though basically similar to those in Cu-based alloys, occurred at different temperatures. The results were unified by recognizing that the phonon wavelengths were the same at corresponding temperature of the anomalies.

I. INTRODUCTION

Recently, Mitchell, Klemens, and Reynolds¹ and Charsley and co-workers²⁻⁴ reported thermal-conductivity measurements of some copper alloys in various stages of deformation. These and other⁵⁻⁷ measurements indicate that the lattice thermal conductivity is not a simple quadratic function of temperature in the range 1.5-4 K as anticipated from standard theory. The reason for this departure from a T^2 dependence is controversial. It has been attributed to (a) a change in the electron-phonon interaction due to short electron mean free paths^{1,8} or (b) a change in the scattering of phonons by the strain fields of nonrandom arrangements of dislocations, such as dislocation dipoles.⁴ In this paper we attempt to resolve the controversy by extending the measurements to lower temperatures (0.5 K) and to other noble-metal hosts (Ag and Au).

In Sec. II the cryostat, measurement techniques, and a test experiment are described. Some considerations of the choice of specimen concentrations and preparation are outlined in Sec. III and the results are presented and discussed in Sec. IV. Section V summarizes our conclusions.

II. EXPERIMENTAL METHODS

The cryostat was similar to one described previously,⁹ with one modification. The ³He pot was moved down, so that the specimen stage, the two vapor-pressure bulbs, and the ³He pot were all on one copper block. Measurements of the thermal conductivity $K(T)$ were made in the steady state by passing a constant heat current Q down the specimen and measuring the temperature difference ΔT between two points. Then

$$K(T) = Q(l/A)/\Delta T, \quad (1)$$

where l is the length between thermometer connections and A is the cross-sectional area of the specimen.

The l/A of each specimen was chosen so that $Q/\Delta T$ at 4 K was similar for all specimens reported here. Thus any anomalies in the results arising from stray heat inputs due to the arrangement of the apparatus should have produced similar effects in all specimens.

Closely matched germanium thermometers (with a resistance R_t of 50 Ω at 4 K and 400 Ω at 0.5 K) were used for measurement of T and ΔT . Copper tags, for the attachment of thermometers, and potential leads (for four-terminal electrical-resistivity measurements) were soldered to the specimen with nonsuperconducting solder. Current, for the four-terminal dc potentiometric arrangement which measured the thermometer resistance, was adjusted to produce negligible heating effects. The power dissipated in the thermometers at all temperatures was less than 4×10^{-8} W. The germanium thermometers were calibrated against the vapor pressure of ⁴He and ³He at temperatures between 0.7 and 4 K. In this range the accuracy of the pressure measurements, made with Texas Instruments precision pressure gauges, corresponded to a temperature uncertainty of 0.1 mK or less and corrections to the pressure readings were kept equally small.

Below 0.7 K, potassium chrome alum crystal-lites mixed with Castolite served as a susceptibility thermometer. The mixture was cast into a $\frac{7}{8}$ -in.-diameter sphere in which the ends of about 300 strands of enamelled No. -38 B & S copper wire were embedded. A removable split Teflon mold

with a hole for the sheaf of wires was used in the casting process. The exposed ends of the wires were then soldered to the specimen station about 2 in. from the salt sphere. The susceptibility of the salt was measured with an arrangement similar to that of Harrison.¹⁰ Between 1.5 and 0.7 K the salt was calibrated against the vapor pressure of ³He. This scale of temperature was extrapolated to 0.4 K using Curie's law.

At least fifty calibration points for R_ρ and T were thus obtained between 0.4 and 4 K and were then fitted to an equation of the form¹¹

$$\ln R_\rho = \sum_{i=0}^n A_i (\ln T)^i. \quad (2)$$

Chebyshev polynomials and double precision were used in the computer calculations for sufficient accuracy. Thus tables for R_ρ at temperature intervals of 0.1 mK were obtained and rapid calculations during the run were possible. Corrections were applied to the calculated temperatures T_{calc} using a deviation curve, $(T - T_{\text{calc}})$ vs T . Since the deviation curves of the two thermometers were very similar, the correction to be applied to the temperature difference ΔT was generally less than 1 mK.

The errors inherent in the apparatus were estimated. Since the electrical power supplied to the specimen heater was easily measured with negligible error and ΔT could be measured to better than 1%, the largest error arose in the measurement of the geometrical factor l/A . However, an error in this factor does not affect the temperature dependence of K . The importance of this error was further reduced since the same geometry was used for the measurement of the electrical resistance $R = \rho(l/A)$, where ρ is the specimen resistivity. Consequently, the Lorenz number L may be experimentally determined by forming the quantity $K\rho/T$ in which the errors in l/A do not appear. Because R contains a small error (0.5%) the Lorenz numbers are estimated to contain errors of the order of 1%, whereas K and ρ values may contain errors as large as 2%.

As a test of the apparatus, a test specimen with known conductivity and with a conductance similar

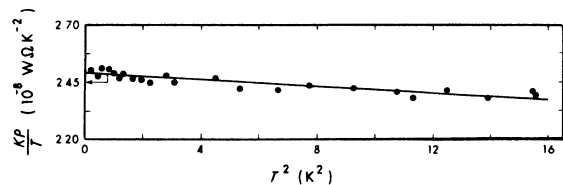


FIG. 1. Plot of the experimental Lorenz ratio ($K\rho/T$) against the square of the absolute temperature T for the pure Pd specimen. The horizontal arrow indicates L_0 .

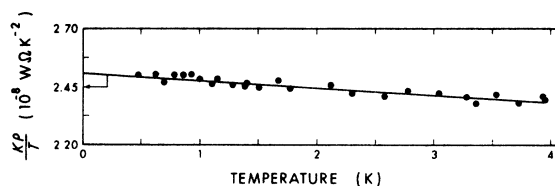


FIG. 2. Plot of the experimental Lorenz ratio ($K\rho/T$) against the absolute temperature T for the pure Pd specimen. The horizontal arrow indicates L_0 .

to the alloys was required. A 1-mm-diam wire of pure Pd (impurity content < 12 ppm) was chosen, since in a pure material; (a) the lattice conductivity could be assumed to be negligible compared to the electronic conductivity and (b) the low-temperature limiting value of the ideal scattering process for electronic conductivity was known from the thorough work of Schriempf.^{12,13} Schriempf's data [Eqs. (1) and (2) of Ref. 12] can be expressed as $K\rho/T = L'_0 - BT^2$, where $L'_0 = 2.48 \times 10^{-8} \text{ W } \Omega \text{ K}^{-2}$ and B depends on ρ_0 . In Fig. 1, $K\rho/T$ for the Pd specimen was plotted against T^2 and fitted by a least-squares procedure, yielding $L'_0 = 2.48 \times 10^{-8} \text{ W } \Omega \text{ K}^{-2}$, which is identical to Schriempf's value.

In Fig. 2, $K\rho/T$ was plotted against T to provide a comparison with the plots for the alloys discussed later. The value for L'_0 , obtained by fitting a straight line to this plot, was different from that of Fig. 1, and incorrect, because the extrapolation had no physical justification. However, the data points fit the line smoothly with small scatter and without any sign of the "bumps" or "kinks" that are apparent in most of the alloy data discussed in Sec. IV.

III. SPECIMENS AND THEIR PREPARATION

The specimens used were fairly concentrated alloys in order to (a) ensure that the electronic component of thermal conductivity was reduced, making it comparable with the lattice component and (b) make the total electrical resistivity practically temperature independent. For practical reasons an important consideration was that the resistance R of the specimen should be almost the same for all alloys. Thus l/A was chosen to make $R \approx 500 \mu\Omega$.

A list of the specimens, along with their residual resistivities and details of annealing procedure, is given in Table I. The specimens were each prepared in a slightly different manner and a brief description of their manufacture follows.

The Cu-10-at.-%-Al alloy¹⁴ was prepared by melting the pure materials in a quartz container, in vacuum, using an induction furnace. The resulting ingot was swaged to produce a rod of 3.6-mm diameter. A cylindrical rod of α -brass (Cu-30%-Zn) $\frac{1}{2}$ in. in diameter was cast in air by Hel-

TABLE I. Details of specimens.

Specimen	Symbol	Residual resistivity ($\mu\Omega$ cm)	Annealing temp. ^a (K)
Cu-10% Al			
cold worked	●	7.54	
first anneal	□	6.79	600
second anneal	△	6.88	675
final anneal	○	6.69	1000
Cu-30% Zn(α -brass)			
cold worked	●	4.59	
first anneal	□	3.82	600
second anneal	△	3.77	700
final anneal	○	3.86	1000
Brass single crystal	●	3.53	
Au-2% Pt			
cold worked	●	1.84	
annealed	○	1.96	1000
Au-10% Ag			
cold worked	●	2.90	
annealed	○	2.71	1000
Ag-2.1% Al			
cold worked	●	3.43	
annealed	○	3.27	1000
Palladium	●	0.061	

^aEach annealing period was 12 h and it was carried out under vacuum except for the brass specimens. They were placed in a hollow cylinder made of the same material and annealed in the presence of argon.

mut Barth.¹⁵ It was swaged down to $\frac{1}{4}$ -in. diameter and specimens 12-cm long and 4-mm diameter were machined from this material. The brass single crystal of 3-mm diameter and 15-cm long was obtained from a commercial source.¹⁶ Seth and Woods¹⁷ prepared the Ag-2.1%-Al specimen which was cold drawn through wire dies with intermediate anneals. The Au-2%-Pt and Au-10%-Ag specimens were prepared by induction melting of 99.999% pure metals in recrystallized alumina crucibles under argon. The ingots were rolled into square rods of about 4-mm² cross section and 10-cm long.

IV. RESULTS AND DISCUSSION

Theoretical background

The thermal conductivity of a metal may be written

$$K = K_e + K_l, \quad (3)$$

where K_e is the electronic component and K_l the lattice or phonon component of the conductivity. The latter is the prime concern of this paper. In a pure metal, most of the heat is transported by the electrons. However, in alloys, because there are point defects, K_e is reduced. At low temperatures, where phonons have long wavelengths, K_l

is not much affected by point defects. Thus in alloys a greater fraction of the heat conduction is due to the lattice, and at temperatures in the helium range, the Wiedemann-Franz-Lorenz law holds, and also the ideal electrical resistivity is negligible compared to the residual resistivity ρ_0 . Then¹⁸

$$K_e = CT, \quad (4)$$

where the constant $C = L_0/\rho_0$ with $L_0 = 2.445 \times 10^{-8}$ W Ω K⁻². From measurements of ρ_0 , K_e may be estimated. Thus measurements of K and estimates of K_e allow K_l to be obtained by applying Eq. (3). Even in annealed specimens K_l is limited by two scattering mechanisms: the scattering of phonons by electrons and by dislocations, respectively represented by the thermal resistances W_{ge} and W_{gd} . Since both these resistivities have the same temperature dependence,¹⁸ the total lattice resistivity can be written

$$W_l = 1/K_l = W_{gd} + W_{ge} \quad (5)$$

and

$$K_l = DT^2. \quad (6)$$

The value of the constant D will depend on the dislocation density in the specimen. Experimental verification of this general behavior has been provided above 2 K.¹⁹⁻²¹

Combining the Eqs. (3), (4), and (6) we obtain

$$K = CT + DT^2, \quad (7)$$

where CT is K_e and DT^2 is K_l . Thus a plot of K/T against T should give a straight line with slope D and intercept L_0/ρ_0 on the K/T axis.

Cu-based alloys

The electrical resistivity of each Cu specimen was found to be independent of temperature from 0.5 to 4 K. However, on annealing, the resistivity assumed a new, temperature-independent value. Table I lists these residual resistivities (ρ_0) and annealing conditions. The K/T vs T plots, described above, for the Cu-10%Al and Cu-30%Zn specimens are shown in Figs. 3 and 4, respectively. Arrowheads pointing to the K/T axes in the figures identify the L_0/ρ_0 for each specimen. In each of the figures the graph with the lowest thermal conductivity (the lowest graph on the plot) corresponds to the specimen in a cold-worked condition. Successive annealing at the temperatures given in Table I produced graphs with higher slopes D . These correspond to higher lattice conductivities indicating that dislocation density was decreased during each anneal. Only for the cold-worked and most-annealed condition of the polycrystalline specimens could single straight lines be fitted to the data above 1.5 K. In other cases a kink occurred in the plot. It is interesting to note

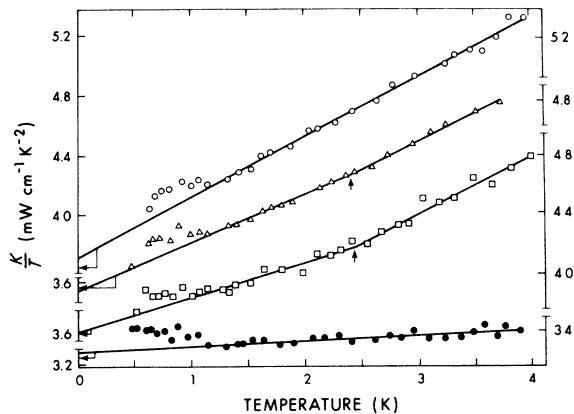


FIG. 3. Ratio of the experimental total thermal conductivity K to the absolute temperature T is plotted against T for the Cu-10% Al alloy. The horizontal arrows indicate the ratio L_0/ρ_0 . The lowest curve represents the specimen in the cold-worked state and each higher curve represents the same specimen in successively higher states of anneal. Annealing conditions are shown in Table I.

that the results shown in Fig. 5 for the single crystal of Cu-30%Zn, in the *as received* condition, exhibit no kink near 3 K and K for this specimen is slightly higher than for annealed polycrystalline specimens.

The presence or absence of kinks has been observed by others. Mitchell *et al.*,¹ in a Cu-10%Al alloy, found that a small kink remained even when the strained specimen was annealed and Friedman *et al.*⁶ reported a similar effect for a Cu-9%Al alloy. Charsley *et al.*³ and Leaver and Charsley⁴ found no kink above 1.5 K in their annealed Cu-12%Al alloys. Similarly, our annealed Cu-10%Al specimen (Fig. 3) showed no kink.

We believe that the explanation for the kinks in annealed specimens is related to the kink being a component of W_{gd} . In those annealed alloys which had the largest K_g , implying smallest W_{gd} , the kink was absent. The argument can be reinforced by examining the partially annealed alloys. The kink, regarded as a discontinuous change in slope, was more extreme in the alloys with more cold work, i. e., greater W_{gd} . The most cold-worked specimen was apparently an exception since it had no kink. However, the slope D was so small that the presence or absence of a kink was unobservable. We therefore disagree with Mitchell *et al.*¹ who ascribed the kink to W_{ge} . Although other large scale defects, which anneal out of cold-worked specimens, could account for our results and the results of other authors, above 1.5 K dislocations seem likely to dominate the phonon scattering in cold-worked specimens.¹⁸

Below 1.2 K an astonishing new feature was ob-

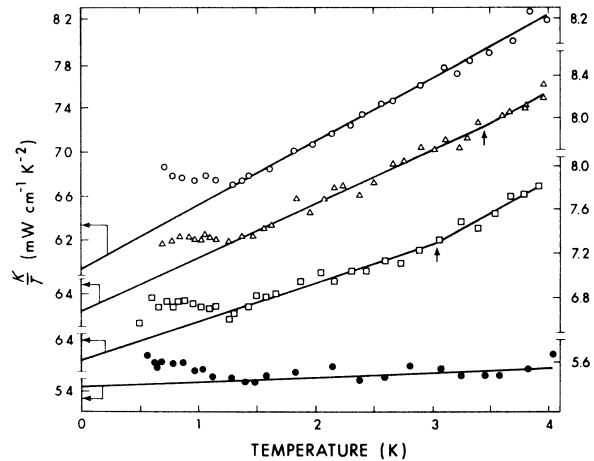


FIG. 4. Ratio of the experimental total thermal conductivity K to the absolute temperature T is plotted against T for the Cu-30% Zn alloy. The horizontal arrows indicate the ratio L_0/ρ_0 . The lowest curve represents the specimen in the cold-worked state and each higher curve represents the same specimen in successively higher states of anneal. Annealing conditions are shown in Table I.

served in both Cu alloys. The thermal-conductivity points were above the line which was extrapolated from high-temperature measurements. Linz (private communication) observed a similar anomaly in his Cu-10%Al alloy. This excess conductivity, subsequently referred to as the "bump," was of similar size in both specimens at all states of anneal and is also believed to be attributable to W_{gd} . The conductivity increase could not be explained by an increase in K_e because a corresponding decrease in ρ , necessary to prevent $K_e\rho/T$ increasing above the classical Lorenz ratio, did not occur. Therefore, unless a conduction process other than phonons or electrons was present, the anomaly must have been in K_g . But, was the excess conductivity related to W_{gd} or W_{ge} ? Since K_g

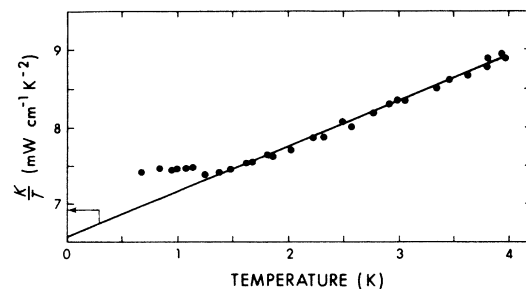


FIG. 5. Ratio of the experimental total thermal conductivity K to the absolute temperature T is plotted against T for the single crystal of brass. The horizontal arrow indicates the ratio L_0/ρ_0 .

in the cold-worked state was very much smaller than in the annealed, $W_{gd} \gg W_{ge}$ in the cold-worked state. The excess conductivity bump persisted in the cold-worked state. This indicated that the bump was a component of W_{gd} and is interpreted as a rapid nonstandard decrease in W_{gd} below 1.2 K. The interpretation is not so straightforward in the annealed alloys since the relative size of W_{ge} and W_{gd} is unknown and the former could be anomalous. The simplest explanation, however, is that W_{gd} was still of measurable size even in the fully annealed state and had the same temperature dependence as for the cold-worked state. Below 0.7 K, K_g/T curves were a much less rapid function of cold work than above 1.5 K. This suggests, for all alloys, that $W_{gd} < W_{ge}$ below 0.7 K. Therefore W_g for the fully annealed alloys should be a good estimate for W_{ge} below 0.7 K. Previous estimates of W_{ge} , based on data above 1.5 K would thus be too small.

To observe whether the bump could be removed, the single crystal specimen (Cu-30%Zn) with, hopefully, a very low concentration of dislocations was obtained. Figure 5 shows that the bump persisted and was similar to that in the annealed polycrystalline specimen (Fig. 4). This result is in agreement with measurements above 1.5 K on a Cu-12%Al single crystal which also had a K_g very similar to an annealed polycrystalline sample of the same concentration.²²

Leaver and Charsley⁴ have calculated the way in which K_g/T might vary with temperature. They used a model in which the dislocation scattering began to diminish at a temperature near 3 K. Here the phonon wavelengths became comparable with a dimension associated with dislocation arrangements (such as dipoles) in which the long-range

fields cancelled. In general the short wavelength phonons "see" the individual dislocations as scattering centers that produce $K_g/T = aT$ and long wavelength phonons see the dipoles as scatterers that produce $K_g/T = bT$ ($b > a$) at much lower temperatures. Thus in our Cu-10%Al and Cu-30%Zn alloys K_g/T may be rising between 3 and 1 K from one linear region to the other. The difficulty with this explanation is that the rise in conductivity in our alloys below 1.2 K was so large, the b/a ratio required seems too large to arise from dislocations associating into dipoles. Calculated curves using this model always underestimate the size of the rise below 1 K. However, it is conceivable that, if a larger number of dislocations were involved in forming networks that acted as single scattering centers for long wavelength phonons, our results could be well reproduced over the whole temperature range from 0.5 to 4 K. Such model calculations would hardly be convincing without more detailed knowledge of the dislocation structure in the alloys.

Au- and Ag-based alloys

Having concluded from the Cu alloy data that the anomalies in K_g were due to a change in the phonon-dislocation scattering, we were interested in reinforcing this conclusion. Consequently we made alloys with the other noble metals as hosts where, due to changes in the Debye temperature, phonon wavelengths would be different and so the anomalies in K_g would, according to Leaver and Charsley's model,⁴ occur at different temperatures.

For each Au and Ag alloy specimen, measurements were made only in highly cold worked and thoroughly annealed states. The electrical resistivity was not measured below 1 K but was found to be independent of temperature between 1 and 4 K in all cases. The ρ_0 values are in Table I. An interesting side issue which arose was that for Au-2%Pt, ρ_0 increased on annealing. This puzzling phenomenon has been observed previously.²³

The K/T vs T plots for Au-2%Pt and Au-10%Ag are shown in Figs. 6 and 7, respectively. In both these alloys the kink occurred near 2 K. The excess conductivity, which was again present in both annealed and cold-worked specimens, appeared below 0.8 K. In Fig. 8, K is shown for Ag-2.1%Al. In this case annealing did not entirely remove the kink which appeared at a temperature well above that in the Au alloys, but was too poorly determined to specify its location relative to the kink in the Cu alloys. The excess conductivity appeared below about 1 K. The arguments we have used to determine the cause of the kink and the excess conductivity bump in Cu alloys also apply to the Au and Ag alloys. Thus we conclude that both kink

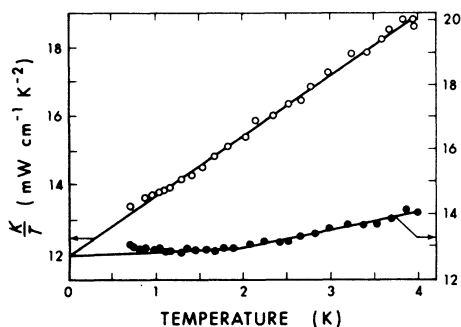


FIG. 6. Ratio of the experimental total thermal conductivity K to the absolute temperature T is plotted against T for the Au-2%Pt alloy. The horizontal arrows indicate the ratio L_0/ρ_0 . The closed circles represent the specimen in the cold-worked state and the scale is given on the right-hand side. The open circles represent the specimen in the annealed state. Annealing conditions are shown in Table I.

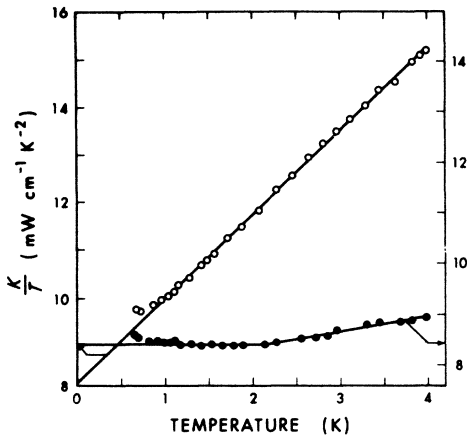


FIG. 7. Ratio of the experimental total thermal conductivity K to the absolute temperature T is plotted against T for the Au-10% Ag alloy. The horizontal arrows indicate the ratio L_0/ρ_0 . The closed circles represent the specimen in the cold-worked state and the scale is given on the right-hand side. The open circles represent the specimen in the annealed state. Annealing conditions are shown in Table I.

and bump occur in W_{gd} .

Due to differences in the mode of introduction of cold work (Sec. III) a different arrangement of dislocations may have occurred in the Au, Ag, and Cu alloys. However, we have evidence for Cu alloys¹⁻⁴ that different methods of introduction of cold work led to the same characteristic kink temperature. Also the excess conductivity bump in our Cu-30%Zn single crystal was practically identical to that of the swaged then annealed poly-

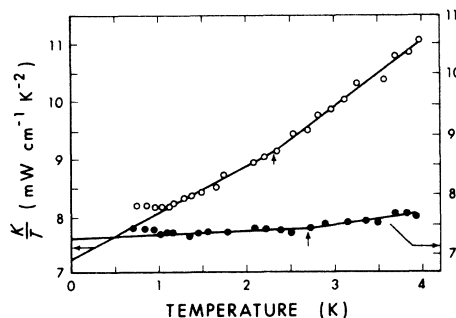


FIG. 8. Ratio of the experimental total thermal conductivity K to the absolute temperature T is plotted against T for the Ag-2.1% Al alloy. The horizontal arrows indicate the ratio L_0/ρ_0 . The closed circles represent the specimen in the cold-worked state and the scale is given on the right-hand side. The open circles represent the specimen in the annealed state. Annealing conditions are shown in Table I.

TABLE II. Effective wavelengths at T_B .

Metal	Θ^a (K)	d^b (Å)	T_B (K)	$\bar{\lambda} = \frac{0.6d\Theta}{T_B}$ (Å)
Copper	344	3.6	1.2	620
Silver	225	4.1	1.0	555
Gold	165	4.1	0.75	540

^aObtained from Ref. 25. ^bObtained from Ref. 26.

crystalline specimen. Thus the differences seem unimportant.

The apparent similarity of K_k for alloys with the same host and the difference between alloys with different hosts can be explained by considering the phonon wavelengths of the hosts. Carruthers²⁴ defined an "effective" wavelength $\bar{\lambda}$ characterizing those phonons most important in conduction at low temperatures by

$$\bar{\lambda} = 0.6d(\Theta/T), \quad (8)$$

where d is the lattice constant and Θ the Debye temperature of the lattice. In Table II values for these quantities have been listed. It may be observed that the effective wavelength is nearly the same in Cu, Ag, and Au at T_B , the temperature immediately below which the excess conductivity appears. The temperature of the kink T_K changes in a similar manner to T_B but since T_K is less well defined than T_B we have not attempted a quantitative estimate. The systematic change in T_B and T_K is further evidence that the lattice conductivity is involved and that the conductivity is limited by scattering centers, characterized by the same separation in each metal investigated.

V. CONCLUSIONS

Measurements of the thermal conductivity K of deformed alloys of copper, silver, and gold confirmed the presence of a nonlinearity or kink in K/T vs T plots near 3 K. In the copper and gold alloys, this kink disappeared when the specimens were sufficiently annealed. There was no evidence of any temperature variation of the electrical resistivity in these alloys below 4 K. We therefore conclude that the kink arose in the lattice conductivity and that it must have been the result of scattering processes that were diminished by annealing.

An excess thermal conductivity, beyond that expected, occurred in each of these alloys below a temperature T_B near 1 K. Although annealing did not remove this excess conductivity it was also ascribed to W_{gd} . Calculations made with a dislocation dipole scattering model suggested by Leaver

and Charsley⁴ could not be made to fit the results in detail, although a modification might. T_B and T_K varied with the host metal of the alloy which suggested that the anomalies in K_L were associated with phonons of the same wavelength in all noble-metal hosts.

ACKNOWLEDGMENTS

We are grateful to Dr. P. G. Klemens and Dr. R. J. Linz for their helpful correspondence and informal discussions. We are also indebted to Dr. Linz for permitting us access to his unpublished data.

*Work supported in part by The National Research Council of Canada.

¹M. A. Mitchell, P. G. Klemens, and C. A. Reynolds, *Phys. Rev. B* **3**, 1119 (1971).

²P. Charsley, A. D. W. Leaver, and J. A. M. Salter, in *Proceedings of the Seventh Conference on Thermal Conductivity*, NBS Spec. Publ. No. 302 (U. S. GPO, Washington, D. C., 1967), p. 131.

³P. Charsley, J. A. M. Salter, and A. D. W. Leaver, *Phys. Status Solidi* **25**, 531 (1968).

⁴A. D. W. Leaver and P. Charsley, *J. Phys. F* **1**, 28 (1971).

⁵M. Kusunoki and H. Suzuki, *J. Phys. Soc. Jap.* **26**, 932 (1969).

⁶A. J. Friedman, T. K. Chu, P. G. Klemens, and C. A. Reynolds, *Phys. Rev. B* **6**, 356 (1972).

⁷A. J. Friedman, *Phys. Rev. B* **7**, 663 (1973).

⁸P. Lindenfeld and W. B. Pennebaker, *Phys. Rev.* **127**, 1881 (1962).

⁹M. A. Archibald, J. E. Dunick, and M. H. Jericho, *Phys. Rev.* **153**, 786 (1967).

¹⁰J. P. Harrison, *Rev. Sci. Instr.* **39**, 145 (1968).

¹¹J. S. Blakemore, J. Winstel, and R. V. Edwards, *Rev. Sci. Instr.* **41**, 835 (1970).

¹²J. T. Schriempf, *Phys. Rev. Lett.* **19**, 1131 (1967).

¹³J. T. Schriempf, *Phys. Rev. Lett.* **20**, 1034 (1968).

¹⁴In the notation used here the host or solvent metal is always named first; the impurity or solute is second.

When an alloy of specific composition is referred to, the concentration of the solute is given in at. %.

¹⁵American Brass and Aluminum Foundry Ltd., 12520 123 St., Edmonton, Alberta, Canada.

¹⁶Windsor Metal Crystals Inc., P. O. Box 331, Westminster, Md., U. S. A.

¹⁷R. S. Seth and S. B. Woods, *Phys. Rev. B* **2**, 2961 (1970).

¹⁸P. G. Klemens, in *Solid State Physics*, edited by F. Seitz and D. Turnbull (Academic, New York, 1958), Vol. 7.

¹⁹G. K. White, S. B. Woods, and M. T. Elford, *Phil. Mag.* **4**, 688 (1959).

²⁰W. R. G. Kemp, P. G. Klemens, and R. J. Tainsh, *Phil. Mag.* **4**, 845 (1959).

²¹J. N. Lomer and H. M. Rosenberg, *Phil. Mag.* **4**, 467 (1959).

²²P. Charsley and J. A. M. Salter, *Phys. Status Solidi* **10**, 575 (1965).

²³J. A. Birch, W. R. G. Kemp, P. G. Klemens, and R. J. Tainsh, *Aust. J. Phys.* **12**, 455 (1959).

²⁴P. Carruthers, *Rev. Mod. Phys.* **33**, 92 (1961).

²⁵W. S. Corak, M. P. Garfunkel, C. B. Satterthwaite, and Aaron Wexler, *Phys. Rev.* **98**, 1699 (1955).

²⁶W. B. Pearson, *A Handbook of Lattice Spacings and Structures of Metals and Alloys* (Pergamon, New York, 1958).